IUST International Journal of Engineering Science,
Vol. 19, No.5-1, 2008, Page 187-198

MODELING OF HEAT TRANSFER AND SOLIDIFICATION OF DROPLET/SUBSTRATE IN MICROCASTING SDM PROCESS

A. Jafari, S.H. Seyedein & M. Haghpanahi

Abstract: *Microcasting Shape-Deposition-Manufacturing is an approach to Solid-Freeform-Fabrication (SFF) process which is a novel method for rapid automated manufacturing of near-net-shape multi-material parts with complex geometries. By this method, objects are made by sequentially depositing molten metal droplets on a substrate and shaping by a CNC tool, layer by layer. Important issues are concerned with remelting dept of substrate, cooling rate and stress build up. In the present study attempts were made to numerically model the heat transfer and phase change within the droplet/substrate, making a better understanding of process performance. Thus, making a brief literature review, a 2-D transient heat transfer Finite Element Analysis was carried out by the use of ANSYS multiphysics, in which solidification is handled using apparent capacity method. Verification was done by available experimental data in the open literature to ensure model predictions. The model was run under various process parameters and obtained results presented in the form of temperature fields, solidification profiles, cooling curves and remelting history curves. Solidification profile studies predict a columnar dendritic solidified structure in the vertical orientation which was in agreement with metallographic sections published earlier. Parametric studied were also carried out under different boundary conditions, initial temperature of the droplet and Substrate temperature. It was concluded that 1) the process is not sensitive to convection/radiation effects from the surface. 2) the main parameter that can control the maximum remelting dept is initial temperature of the droplet. the more drop temperature, the more remelting dept. This parameter also affects cooling rate during solidification. 3) Increasing substrate temperature showed a decreased cooling rate in solid, which can be used to reduce residual stresses, but it had a minor effect on the cooling rates during solidification.*

Keywords*: Heat Transfer, Solidification, FEM, Shape Deposition Manufacturing, Microcasting*

1. Introduction

Solid Freeform Fabrication (SFF) processes allow a Computer Aided-Design (CAD) model of a part to be transformed into a three-dimensional shape by cutting the CAD model into slices and building the part layer by layer from the slices. The application of SFF processes is in rapid prototyping, to create a nonfunctional model of the part shape, where layers are built up by successive polymer curing (e.g., stereo lithography) or by successive deposition of molten polymer (e.g., Fused Deposition Modeling). Efforts have recently been focused on extending SFF methods to produce functional prototypes or final parts out of engineering materials. The benefits of using SFF processes is the ability to build parts with complicated geometries, internal cavities, multiple materials and embedded components, and to build them in an automated way, based on a CAD representation of a three-dimensional shape. Although melting and fusion techniques vary, most direct manufacture SFF processes involve successively applying droplets of molten material to form a layer. Processes of this type include Laser Engineered Net Shaping (LENS), Directed Light Fabrication (DLF) (Los Alamos), Direct Selective Laser Sintering (SLS) and Shape Deposition Manufacturing (SDM) [1, 2].

Shape Deposition Manufacturing (SDM) systematically combines the benefits of SFF with other intermediate processing such as CNC machining for accuracy and precision with good surface quality. In SDM, objects are

Paper first received July. 10, 2007 and in revised form July. 12, 2009.

A. Jafari, *PhD student, School of Metallurgy and Materials Engineering, Iran University of Science and Technology (IUST), aminjafari57@gmail.com*

S.H. Seyedein *Associate Professor, School of Metallurgy and Materials Engineering, Iran University of Science and Technology (IUST), seyedein@iust.ac.ir*

M. Haghpanahi *Associate Professor, Dept. of Mechanical Engineering, Iran University of Science and Technology, IUST.,*

incrementally built-up using a combination of layered material deposition and removal as shown in Fig. 1. With SDM, several types of materials can be deposited including metals, plastics and ceramics [3].

In Laser SDM or the LENS process, parts are constructed by focusing a high-power laser beam onto a metal substrate, where streams of metallic powder are simultaneously injected. The laser locally melts the powder to form a molten pool on the surface of the growing part. By moving the laser beam, parts are built up, line by line and layer by layer [4, 5].

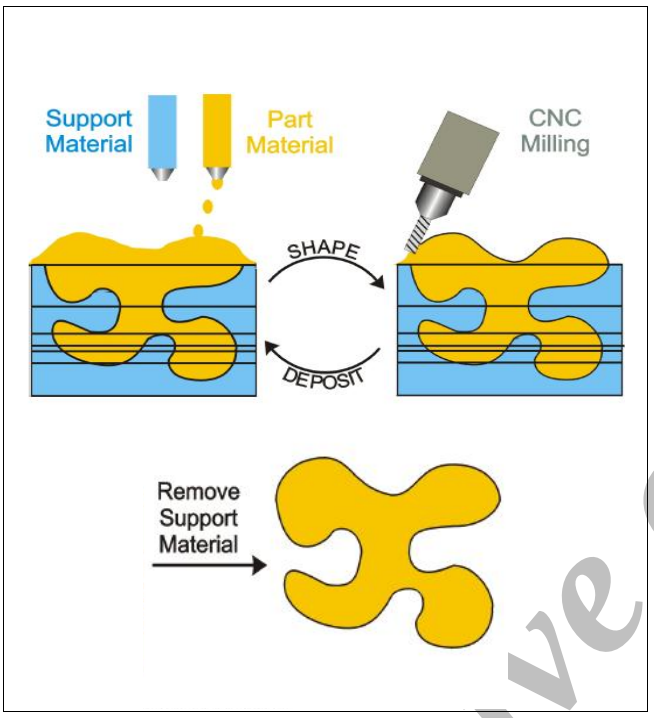

Fig. 1. Microcasting Shape-Deposition-Manufacturing (SDM) [6]

In microcasting SDM, individual layers are deposited by individual droplets of superheated molten metal. Layers are then accurately machined to net shape before depositing additional material. Fig. 2a shows the microcaster assembly which consists of a plasma-welding torch, a wire feeder and a shroud. The plasma-welding torch is positioned horizontally and the wire feeder is positioned vertically, as schematically shown in Fig. 2b. An electric arc is established between the welding torch and the feed wire to generate plasma. The wire is fed into the plasma and is melted to form superheated droplets. The droplets fall several centimeters and strike the substrate with a velocity of the order of one meter per second, depending on the plasma gun stand-off distance [6]. The shroud surrounds the area where the plasma torch and the wire feeder meet. Nitrogen flows through the shroud to create an inert atmosphere around the falling metal droplets to prevent oxidation. The robot arm moves the microcaster assembly over the substrate, depositing individual droplets of superheated molten metal in a prescribed pattern to form rows and layers. Due to the large volume-to-surface ratio, the droplet remains superheated in flight and, at impact, contains sufficient thermal energy to locally remelt the underlying substrate to attain metallurgical bonding upon solidification [3].

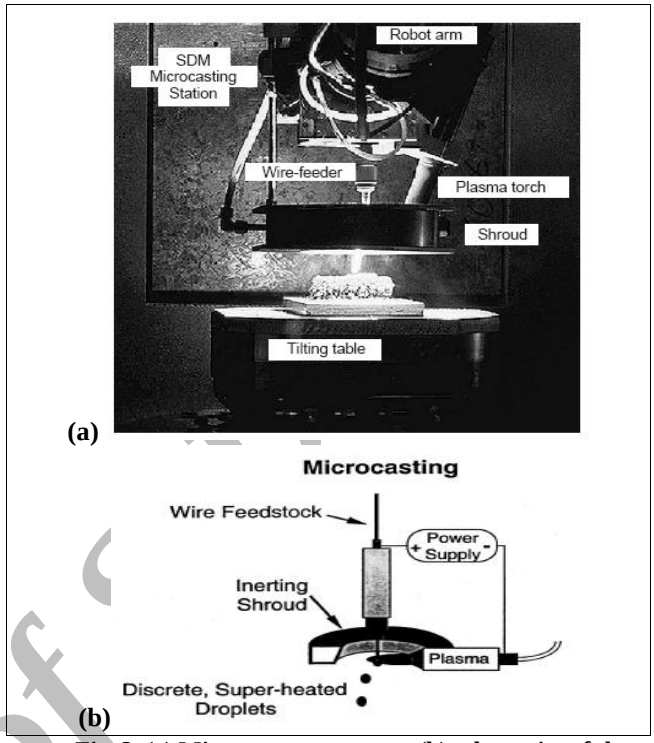

Fig. 2. (a) Microcaster apparatus (b) schematics of the plasma torch and microcasting process [1]

As an example of multimaterial tooling, copper can be embedded within a stainless steel part (to exploit its higher thermal conductivity for molding applications, for instance). Copper can also be used as a scarifying support material during construction, and subsequently etched away in a solution of nitric acid (Fig. 3) [1].

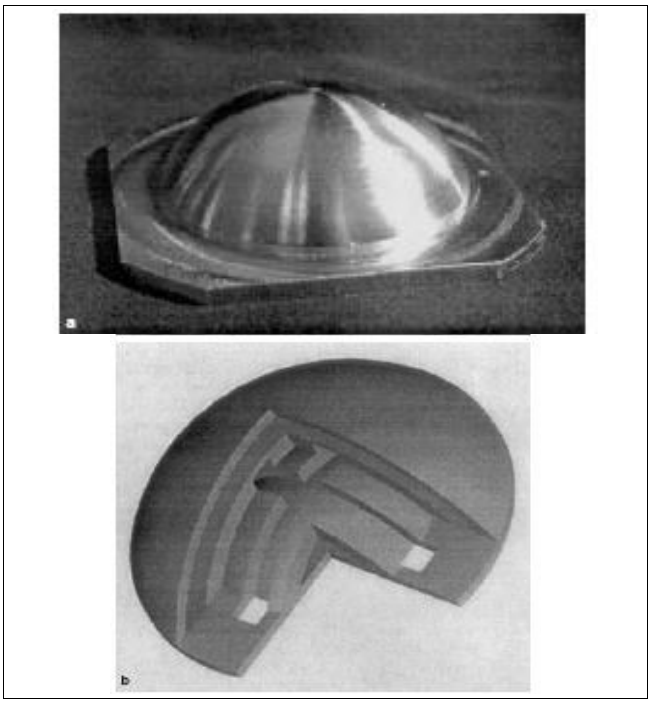

Fig. 3. (a) Manufactured part by microcasting (b) CAD representation of the part [1]

Optimizing the microcasting SDM process requires the determination of the effects of the process parameters on the final quality of the manufactured part. Important issues toward the production of high quality objects are the control of substrate remelting depth and cooling rate during solidification. Substrate remelting determines the extent of metallurgic bonding between deposited layers. High quality bonds between layers are required for the strength and integrity of the final part because the artifact has to withstand residual thermal stresses induced by the large initial temperature difference between the droplet and the substrate. On the other hand, excessive heat and remelting are to be avoided to reduce the accumulated residual stresses and to preserve the quality of the exterior surface of the part. Controlling the deposition material cooling rate during solidification is also important because it determines the final microstructure and material properties. In addition, good flow characteristics of deposited droplets are sought to avoid the presence of voids and to obtain fully dense and homogeneous artifacts; therefore, controlling the droplet solidification time is also of concern [3, 7].

Schmaltz and Amon [8] presented a brief descriptions of the thermal modeling approach, the numerical prediction of the cooling rates and substrate remelting depths of steel deposited on steel and on copper, and the analytical and experimental methods used to verify temperature histories and useful information was obtained in the selection of operating parameters during the manufacture of microcast artifacts. Amon et al [9] investigated a molten metal droplet landing and bonding to a solid substrate with combined analytical, numerical, and experimental techniques. Numerical results indicate that droplet to substrate conduction is the dominant heat transfer mode during remelting and solidification. Furthermore, a highly time-dependent heat transfer coefficient at the droplet/substrate interface necessitates a combined numerical model of the droplet and substrate for accurate predictions of the substrate remelting. Chin, Beuth and Amon [10, 11] quantified the effect of substrate preheating on residual thermal stresses. They also modeled the deposition of a second droplet and assessed the effect on residual stresses of localized preheating by the first deposited droplet. They found that the more computationally efficient 1D models aid in interpreting the 2D results and provide reliable estimates of maximum stress magnitudes.

By another research Amon et al [7] presented an overview of thermal and mechanical issues associated with SDM and microcasting, including the control of interlayer metallurgical bonding through substrate remelting, the control of cooling rates of both the substrate and the deposited material and the minimization of residual thermal stress effects. Schmaltz and Amon [6] predicted the position of the remelting and solidification fronts. They also modeled the effect of the convection induced by the droplet spreading through a time-dependent effective thermal conductivity. High speed filming of the molten droplet impinging and spreading on the substrate is performed to obtain the required parameters to determine this time dependent effective conductivity. Schmaltz and Amon [3] then particularly investigated the effect of droplet impinging temperatures, substrate initial temperatures and combinations of copper and stainless steel materials. Their numerical predictions reveal that impinging droplet temperature has a minimal effect on the cooling rates during solidification, While it has a significant effect on the substrate remelting depth.

They quantified the extent to which substrate preheating lowers the cooling rate during solidification and promotes substrate remelting. The study of the interaction between copper and stainless steel materials shows that the cooling rates and the substrate remelting are both highly dependent on the combination of materials. Kovacevic et al [12] presented a foundation for developing a new technique based on controlling the heat and mass transfer processes in gas metal arc welding. They found that to accurately control the resultant shape of the part, as well as its mechanical and metallurgical properties, the drop size and detachment rate must be precisely controlled. Chandra and Park [13] performed an experimentation to study coalescence of molten tin droplet deposited on an aluminum plate that was moving horizontally. They could successfully produce continuous beads when the substrate temperature was kept above 175°C and droplets overlapped by a distance equal to half their diameter.

Carter [14] has given an overview of currently available capabilities in the Rapid Prototyping industry. Capabilities and limitations of the most popular rapid-prototyping machines are presented. Criteria for choosing a process are presented, then specifications of popular machines are given in a table, including estimated costs.

Kovacevic and Jandric [15] found that the building of a three-dimensional part by welding is especially sensitive to inadequate heat input. Manually adjusting the heat input cannot be used because of the dynamic changes in the underlying substrate geometry. To investigate this problem a Finite Element Analysis has been done that correlates the influence of the different underlying substrate geometry to the quality of the welding-based deposition process and the results suggested that influence of the geometry is significant. They also proposed a real-time adaptive controller of the welding parameters that performs heat management according to the volume changes of the material of the underlying layers in the vicinity of the heat source. Sahu et al [16] have recently described a mathematical model to predict thermal history and solidification behavior of atomized droplets of aluminum, copper and nickel in spray deposition.

Their model estimates nucleation temperature, nucleation position and the extent of droplet solidification during flight. They have discussed the influence of the type of metal, atomizing gas, deposition distance, different gas velocity correlations and droplet size on solidification characteristics. Several other attempts [2, 4, 17-20] have been made to investigate the effects of residual stresses

and thermomechanical modeling as an important issue in microcasting SDM which are to be reviewed elsewhere. Several other works have been done about different aspects of the process. [26-32].

The purpose of the present study was to perform a 2-D Finite Element Analysis, which may give helps to make a better understanding of the process, concentrating attention to the solidification/remelting and resultant structure, which determines the final material properties and probable defects as well as affecting process performance, which is not properly addressed in details, earlier. By the first work, attempts were concentrated on literature review, model development and mainly make a better understanding of the remelting/solidification phenomena during the process. Therefore experimental observations are to be carried out as a separate study, and for now, required data were adopted from results obtained by other researchers.

2. Mathematical Model

As previously discussed a molten droplet falls down and strikes a relatively large substrate in the form of a hemispherical cap at time $t = 0$. Physical phenomena which are to be taken into consideration are the heat transfer by conduction and convection within the droplet, solidification and remelting and solidification of the substrate. There also may be probable solid state phase changes (in the case of carbon steel) which sensibly affects the heat transfer during the remelting of the substrate. For the issue of the droplet geometry, it may be accepted that; while different geometries, generally like a hemispherical cap, would have almost the same contribution to the substrate remelting, several numerical CFD efforts is needed to consider the impingment and the geometry evolution of the drop. According to the objectives and main interested aspects of the process, some assumptions were made in mathematical description of the process:

- The substrate is a cylinder, where an axisymetrical plane of droplet and substrate can represent the 3D phenomena of the interest. (Fig. 6)
- The droplet does not change in shape during cooling and solidification and has a hemi-spherical cap shape.
- The heat transfer within the steel is affected by the latent heat release of the solidification and some solid state structure changes.
- The heat transfer interactions between the material and environment are controlled by heat convection and radiation
- The drop and the substrate are in a perfect contact.

2.1. Governing Equation

Based on heat transfer in axisymmetric cylindrical coordinates and with the above assumptions, the governing equation of the model can be written as follow [24]:

$$\frac{\partial\left(\rho c_{\text{eff}} T\right)}{\partial t} = \frac{1}{r}\frac{\partial}{\partial r}\left(k_{\text{eff}}\, r \frac{\partial T}{\partial r}\right) + \frac{\partial}{\partial z}\left(k_{\text{eff}} \frac{\partial T}{\partial z}\right) \qquad (1)$$

Where T is the temperature, ρ is density and k_{eff} and c_{eff} are, respectively, the effective heat conduction and heat capacity of steel. k_{eff} and c_{eff} are introduced to include convective heat effects and latent heat of phase change, respectively, as well as the thermophysical properties of the material. These parameters are explained and quantified in the follow.

2.2. Modeling of convective heat transfer

The heat flux vector within the molten droplet is formulated by conductive and convective heat flux vectors as [24]:

$$\mathbf{q}_{\text{eff}} = \mathbf{q}_{\text{conv}} + \mathbf{q}_{\text{cond}} = \rho\, \mathbf{u}\, c T - k \nabla T \qquad (2)$$

where $\mathbf{q}$'s are the heat flux vectors, ρ is density, c is heat capacity, k is thermal conductivity and $\mathbf{u}$ is the velocity vector field within the molten droplet. From the above formulation, calculation of $\mathbf{u}$ requires considerable numerical efforts which may be out of practical issues with the microcasting SDM process. [6] As proposed by Flemings [20] the conductivity of the melt can be multiplied by a factor, greater than one, to effectively include the convective heat flux. Thus equation (2) can be replaced by:

$$\mathbf{q}_{\text{eff}} = -k_{\text{eff}} \nabla T \qquad (3)$$

Trying to analytically calculate the conductivity multiplier, K_{factor}, Amon et al [6] estimated the Nusselt number and the thickness of the thermal boundary layer for stainless steel droplets based on (a) the typical droplet sizes and (b) the impinging velocity. They obtained a conductivity multiplier of 3.2 for the droplets. They also tried a method of inverse modeling by the use of their heat transfer model and experimental measurements. In the present study data used by Brimacombe et al [21] in continuous casting of steel were adopted for effective heat conductivity.

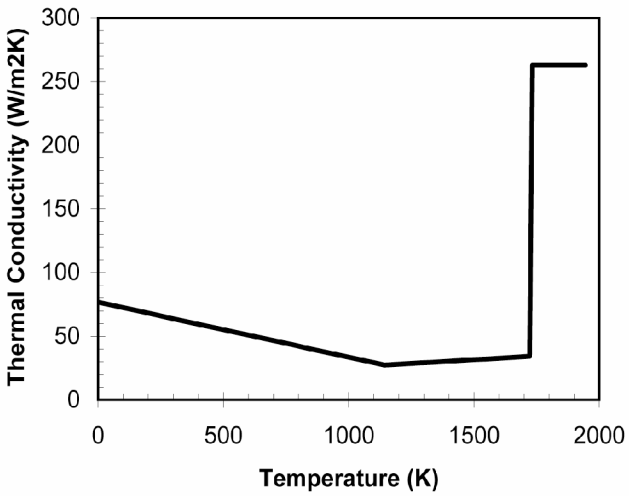

Fig. 4. Effective thermal conductivity of the carbon steel [21].

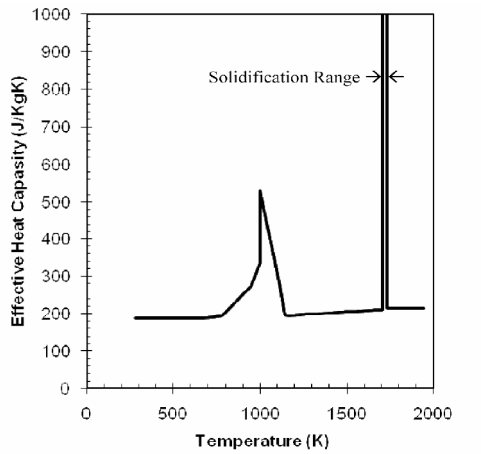

Fig. 5. Apparent heat capacity of steel which contains the latent heat of solidification [21]

2.3. Modeling of Phase Changes

When the molten droplet deposited on a substrate, the substrate starts to extract the superheat of the droplet. Consequently, depending on the ability of substrate to distribute the superheat within its bulk (conductivity), it would have a locally increase in temperature just below the droplet. In the microcasting SDM, it is preferred to have a localized remelting in the substrate for bonding. In this case, the extracted heat is consumed for a locally solid $\rightarrow$ liquid phase change in the substrate, instead of more increase in temperature. After a short while, there will be no more superheat, when the substrate starts to extract the latent heat of the melt. Again it causes a phase change of, this time, liquid $\rightarrow$ solid. In addition to remelting and solidification, the solid material will experience other changes in lattice structure which can sensibly affect the heat transfer. The Lattice of the different solid phases takes the different levels of energy. to handle these phase change effects within the energy equation (1), one can adopt the apparent heat capacity method by which an apparent heat capacity is introduced as a function of temperature so that the area under its curve contains both sensible heat and latent heat, regarding to the phase diagram as well as specific heat capacity of the material. It is notable that when a material (especially metals) experiences a heating/cooling process, different process conditions may push the material toward different structures, based on kinetics of transformations. (e.g. in molten metals, very high cooling rates would results in amorphous structures, where there would be no latent heat release as known in the solidification [20]). Therefore the material does not always obeys only one predefined path, So that it may significantly affect the considered heat transfer routine as well as material properties. Similar issue is referred for copper alloys [22]. High cooling rate during solidification of copper increases the concentration of non-equilibrium vacancies, which significantly changes the specific heat capacity and latent heat of fusion of copper. Here in the process of cooling steel, the same issue may be arisen because of martensitic transformation in steels, which is to be investigated properly in a separate study.

The enthalpy of the phase i can be written as:

$$\mathrm{d}h_i = c_i\,\mathrm{d}T \;\Rightarrow\; h_i = h_i^{\circ} + \int_{T_{\mathrm{ref}}}^{T} c_i \mathrm{d}T \tag{4}$$

$$\Delta h_{1\to 2} = \Delta h_{1\to 2}^{\circ} + \int_{T_{\mathrm{ref}}}^{T} \Delta c_{1\to 2}\mathrm{d}T \tag{5}$$

$\Delta h_{1\to 2}$ is the enthalpy of phase change. If the two phase are assumed to have a same value of heat capacity, the second term in Equation (5) will be omitted. Thus, $\Delta h_{1\to 2} \approx \Delta h_{1\to 2}^{\circ}$, which may be addressed as the latent heat of fusion. Now, the apparent heat capacity can be derived by differentiating Equation (5) with respect to temperature as follow:

$$f_1 + f_2 = 1 \tag{6}$$

$$c_{\mathrm{eff}} = \frac{\mathrm{d}h_{\mathrm{m}}}{\mathrm{d}T} = \frac{\mathrm{d}h_1}{\mathrm{d}T} + \frac{\mathrm{d}\left(f_2 \Delta h_{1-2}\right)}{\mathrm{d}T} \approx c + \Delta h_{1-2}\frac{\mathrm{d}\,f_2}{\mathrm{d}T} \tag{7}$$

Where f is the mass fraction of the phases (here subscripts 1 and 2 used for liquid and solid phases, respectively). Now, the extra unknown, f, can be treated by coupling the f and T from the thermodynamics of the phases, introducing an extra algebraic equation to the system. The most common case is when the volume fraction, f, is assumed to vary in the mushy temperature range, linearly [23]. Therefore the term $\mathrm{d}f/\mathrm{d}T$ in equation (7) is simply derived as $1/\Delta T$, where ΔT is the difference between the solidus and liquidus temperatures. Thus, the apparent heat capacity would be written as:

$$c_{\mathrm{eff}} = \begin{cases} c & T < T_{\mathrm{S}} \\ c + \dfrac{\Delta H_{\mathrm{f}}}{\Delta T} & T_{\mathrm{S}} \le T \le T_{\mathrm{L}} \\ c & T > T_{\mathrm{L}} \end{cases} \tag{8}$$

Fig. 5 shows the adopted c_{eff} as a function of temperature, in which the solidification of steel is included and some heat effects of solid state phase changes as well.

2.4. Boundary Conditions

Fig. 6 demonstrates the calculation domain and boundary conditions applied. As mentioned before, the problem assumed to be axisymmetric. The left side of the domain shown in Fig. 5 is the axis of symmetry, where no radial heat flux can pass across the boundary. The bottom side of substrate maintained at a fix temperature of initial conditions, because the bulk of the substrate will efficiently act as a semi-infinite medium. From the other sides, the droplet and the substrate surfaces are in contact with the ambient fluid, where a combination of forced convection (Nitrogen flow) and radiation, extracts heat from the domain. Finally, the boundary condition applied to these surfaces can be summarized in the following form:

$$\begin{aligned} \mathbf{q} &= \mathbf{q}_{\mathrm{convection}} + \mathbf{q}_{\mathrm{radiation}} \\ &= h\left(T_{\mathrm{S}} - T_{\infty}\right) + \sigma\varepsilon\left(T_{\mathrm{S}}^4 - T_{\infty}^4\right) \\ &= \left[h + \sigma\varepsilon\left(T_{\mathrm{S}}^2 + T_{\infty}^2\right)\left(T_{\mathrm{S}} + T_{\infty}\right)\right]\left(T_{\mathrm{S}} - T_{\infty}\right) \\ &= h_{\mathrm{total}}\left(T_{\mathrm{S}} - T_{\infty}\right) \end{aligned} \tag{9}$$

The emmisivity, ε, was adopted from tabulated values for steel surface [24]. The value of h_{total} is calculated as a function of surface temperature, which is shown in Fig. 7.

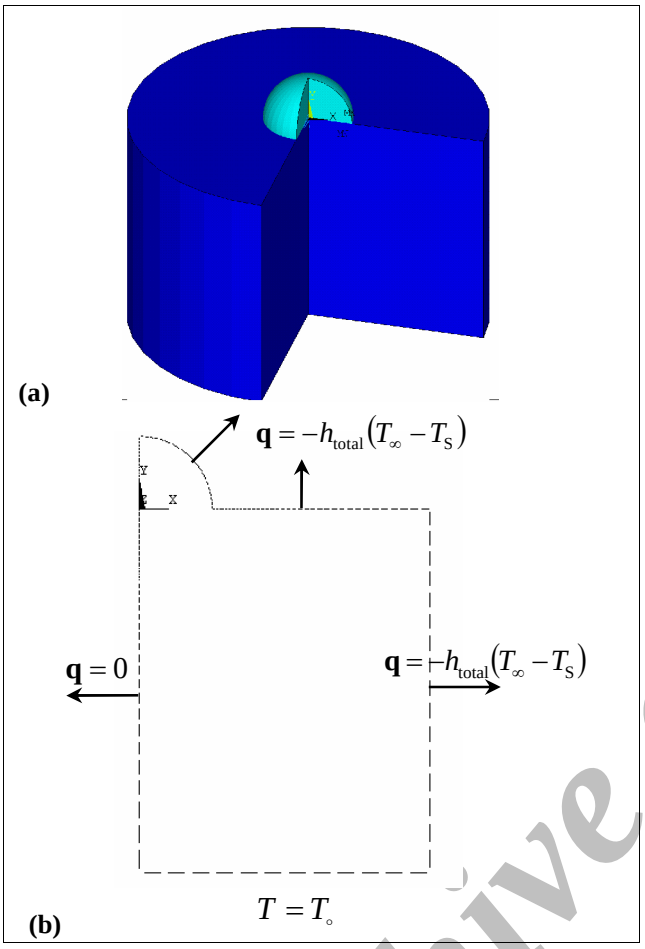

Fig. 6. Schematic of the domain and the boundary conditions.

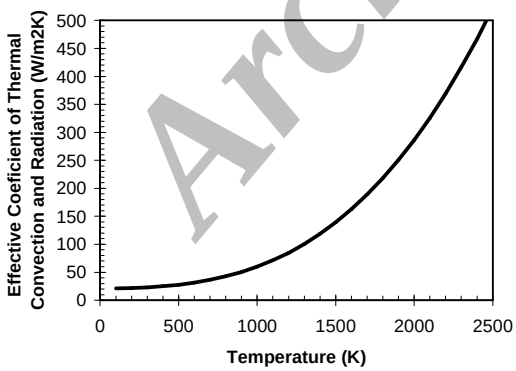

Fig. 7. Calculated heat transfer coefficient for convection and radiation. [24]

2.5. Initial Conditions

It is assumed that at time t = 0 the droplet has a uniform temperature of T_i and the substrate is preheated to the temperature of T_o as well. T_i and T_o can be manually adjusted in the microcasting SDM process, which may be the most important parameters that are to be studied.

3. Numerical Methodology

The general form of the governing equation (Equation 1) can be written as [25]:

$$\lambda\frac{\partial\phi}{\partial t} = \frac{1}{r}\left[D_r\frac{\partial}{\partial r}\left(r\frac{\partial\phi}{\partial r}\right)\right] + D_z\frac{\partial^2\phi}{\partial r^2} + Q \qquad (10)$$

Using Galerkin method and substitution of the shape functions of the elements gives the algebraic equations of the weighted residual Integral for equation (10) as follows [25]:

$$\left\{R^{(e)}\right\} = [C]\left\{\dot{\Phi}^{(e)}\right\} + [K]\left\{\Phi^{(e)}\right\} + \left\{I^{(e)}\right\} - \left\{f_Q{}^{(e)}\right\} \qquad (11)$$

Where the Capacitant matrix, $[C]$, and Stiffness matrix, $[K]$, respectively, are:

$$[C] = \int_V \lambda[N]^T[N]dV \qquad (12)$$

$$[K] = \int_V [B]^T[D][B]\,dV\,, \quad [B] = [L][N] \qquad (13)$$

Where $[N]$ is the shape function of the elements and $[B]$ is the derivative matrix of $[N]$. Other interelement relation and boundary condition matrix, $\left\{I^{(e)}\right\}$, is [25]:

$$\left\{I^{(e)}\right\} = -\int_\Gamma [N]^T\left(D_r\frac{\partial\phi}{\partial r}\cos\theta + D_z\frac{\partial\phi}{\partial z}\sin\theta\right)d\Gamma \qquad (14)$$

And finally the source matrix, $\left\{f_Q{}^{(e)}\right\}$, is:

$$\left\{f_Q^{(e)}\right\} = \int_V Q[N]^T\,dV \qquad (15)$$

Based on Finite Element Method, ANSYS multiphysics was used for grid-generation, numerical calculation and solving equations. The domain was discretized by axisymmetric quadrilateral elements, known as PLANE75 in the software. Fig. 8 shows the arrangement and size of the generated mesh. As can be seen a fine non-uniform mesh density was used according to the rapid nature of the process, high temperature gradients (especially near the droplet/substrate interface) and nonlinearity due to phase change.

Tab. 1. Parameters used for the numerical modeling.

Material Properties (carbon steel)		
ρ	Kg/m^3	7800
c_P	J/KgK	Fig. 5 (includes latent heat)
k	W/mK	Fig. 4 (includes heat flow effect)
T_L	K	1733
T_S	K	1704
Δh_f	KJ/Kg	200
Process Parameters		
R_{drop}	mm	3
$R_{substrate}$	mm	12
$H_{substrate}$	mm	15
T_{drop}	K	2500, 2200, 2000, 1800
$T_{substrate}$	K	30, 60, 100, 150
T_{atm}	K	30

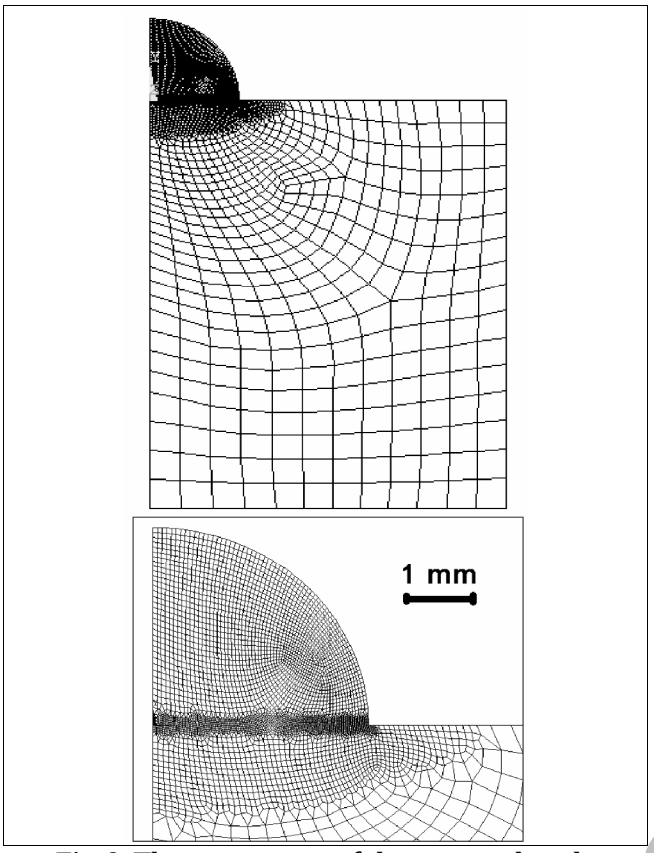

Fig. 8. The arrangement of the generated mesh.

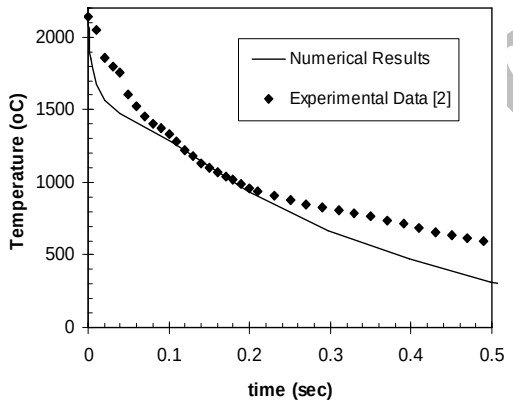

Fig. 9. Numerical temperature history curve in comparison with experimental datd.

Equation (8) was used to introduce the latent heat release during the phase change into the ANSYS solver, by the use of input nonlinear material properties. It should be noted that in the apparent capacity method for handling the phase change, cares must be taken for element sizes and time steps so that the nodal temperatures does not jump over the mushy region, where the latent heat appears. Therefore, a time step of 10^{-3} sec was chosen, which can be fined as low as 10^{-10} sec. Table 1. shows the parameters used in the model.

4. Results and Discussions

4.1. Verification

To verify the FEM model, the numerical results in the form of temperature history curves was compared with experimental data obtained by Amon et al [1], which is shown in Fig. 9. Reasonable agreement was obtained, while differences can be seen because of probable dissimilarity in input parameters, such as dimensions of substrate and/or material properties.

4.2. Temperature Fields and Solidification Profiles

Temperature distribution within the droplet and substrate was obtained during microcasting SDM under various process conditions. Fig. 10 shows a typical temperature field as a function of time. As shown in the Fig., at time $t = 0$ the droplet has a temperature of 2200 °C and the substrate maintained at room temperature (30 °C). As soon as the process starts, a high temperature gradient at droplet/substrate interface leads to a rapid heat transfer from the droplet to the substrate. After a short while the substrate damps the heat content of the droplet which is followed by a local heating below the droplet at first, and cooling down the whole system later. The droplet is also cooled by the environment through convection and radiation from surface. Although later, it will be shown that the convection and radiation heat effects could be ignored in comparison with conduction and solidification effects. The heat transfer is controlled by solidification/remelting of the droplet and substrate material as well as heat conduction within them. Solidification also determines the final structure and properties of the metal part. Thus, Solidification profile can help to predict structure and probable defects. Therefore, solidification profiles during microcasting SDM process were also determined for different process conditions. Fig. 11 shows a successive solidification process and phase regions. In this Fig., the dark color shows solid area and the light color demonstrates liquid metal. At time t = 0, the liquid droplet is located on a solid substrate at room temperature. Then, remelting of substrate takes place up to four stages later. An intermediate color in Fig. 11 between liquid and solid regions shows the development of a mushy region. From the high temperature gradient in vertical direction and remelting of substrate, it could be surly said that the mushy region contents large columnar dendrites along vertical direction, which origin from half-melted grains in the substrate and grow through the molten droplet. Such a condition is very common in welding process [ASM handbook].

This mechanism leads to a directional solidification and a directional columnar structure, consequently. Fig. 13 shows a photograph of a typical metallographic section prepared by Amon et al [6] which presents a vertical columnar structure as well as remelting dept in the substrate. In This structure micro-cracks with a vertical orientation are more common than other directions. Another issue is concerned with the thickness of the mushy region. During the solidification of the bottom of the droplet, a thin mushy thickness can be seen. But, with some progress of solidification front, the mushy region becomes larger (Fig. 11), where there is a probability of the generation of microsegregation and shrinkage voids between secondary dendrite arms.

4.3. Parametric Study

In order to investigate the sensitivity of the process to radiation and convection effects, model was run under different heat transfer coefficient at boundaries (Fig. 7). Fig. 13 shows three cooling curves for the top of the droplet, one for about free convection plus radiation (h_{conv} = 20 W/m^{2}K), another for a week forced convection plus radiation (h_{conv} = 50 W/m^{2}K), and the other for free convection without radiation. The results show ignorable difference, indicating a poor sensitivity of the process to radiation and convection effects. For investigation the effect of initial temperature of the droplet on the process performance, four different drop temperatures of 1800, 2000, 2200 and 2500 °C were chosen. The model was run for the selected drop temperatures with constant other parameters. Then temperature history curves at different location of the droplet were extracted from the obtained results. Fig. 14 show the cooling curves and the positions at which temperature histories are plotted. A rough comparison between Fig.s 14a to 14b can give a sense for cooling process at different points within the droplet. In Fig. 14c and 14d, the flat step in cooling curves shows the solidification time for the top and middle points which can not be seen in Fig.s 14a and 14b, while they show a high cooling rate with a rapid solidification in the basal points of the droplet. By the use of proper phase transformation data such cooling curves would help to predict macrostructure within the solidified droplet.

In addition to the solidification region in Fig.15a to Fig.15d, there is another slope discontinuity about 850 °C which is more visible in Fig. 14d, It is because of the phase transformation effects in heat transfer process, which is included by an apparent heat capacity (Fig. 5). For investigations of the macrostructure development and its effects on the heat transfer process as well as stress field, more studies and data are needed which is to be worked on as another research. Increasing initial temperature of the droplet causes a slight upward shift in the first half of the cooling curves (as it also mentioned by other researchers [3]). So that there is no change in second half as well as in final temperature. To study the effects of substrate temperature, the initial temperature of the droplet is fixed at 2200 °C and the model was run for four different substrate temperatures of 30, 60, 100 and 150 °C. The cooling curves at interested locations are extracted from the results. Those are shown in Fig. 15. As can be seen in the graphs, again, the location is the dominant factor that determines the trend of cooling curves. So that Fig. 14a-14d are similar to Fig. 15a-15d, respectively. Increasing substrate temperature also shifts the cooling curve upward, but this time in the second half of cooling curves as well as final temperature. It is clear that substrate temperature has no sensible effect on temperature history during solidification.

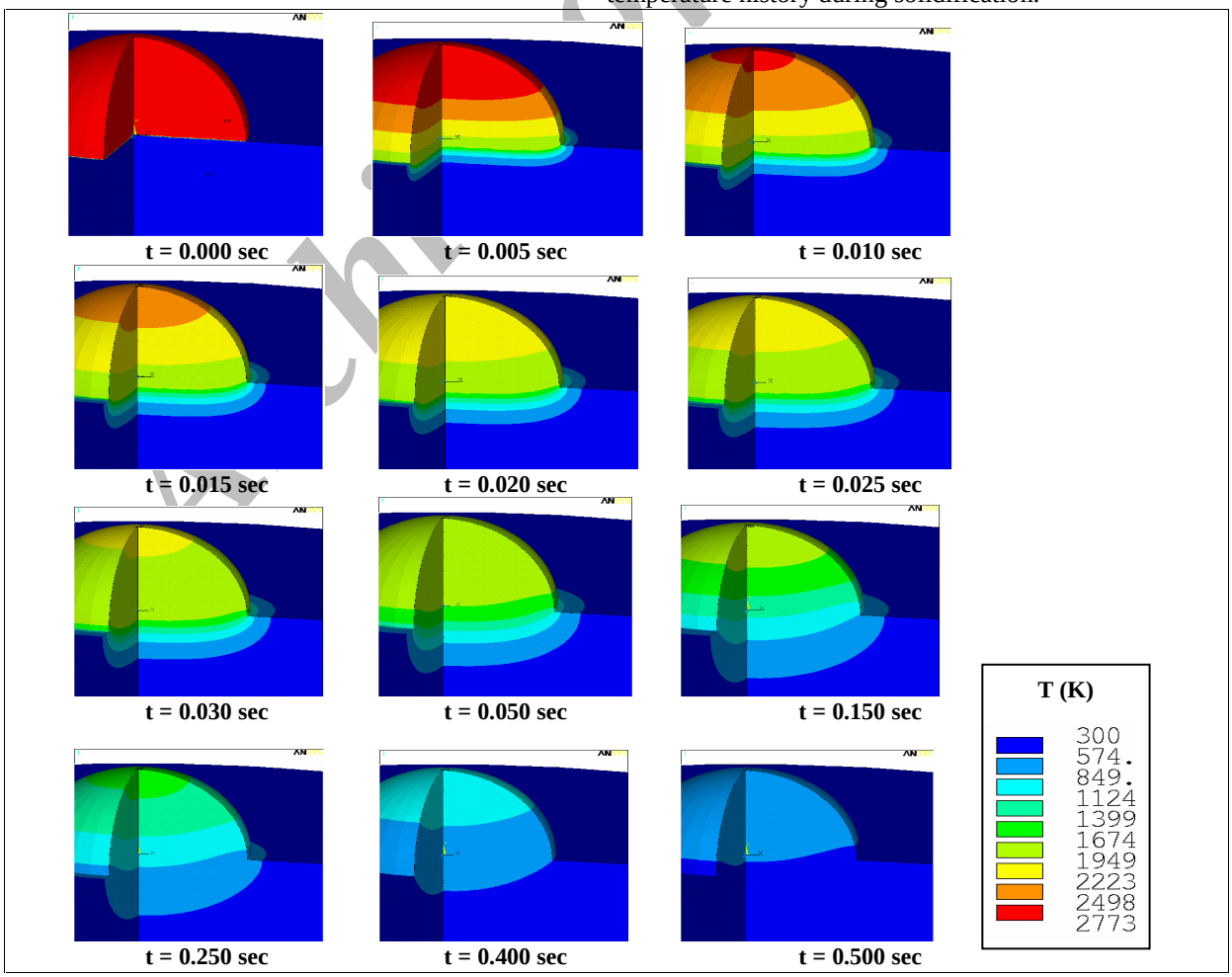

Fig. 10. Typical temperature distribution during microcasting SDM process.

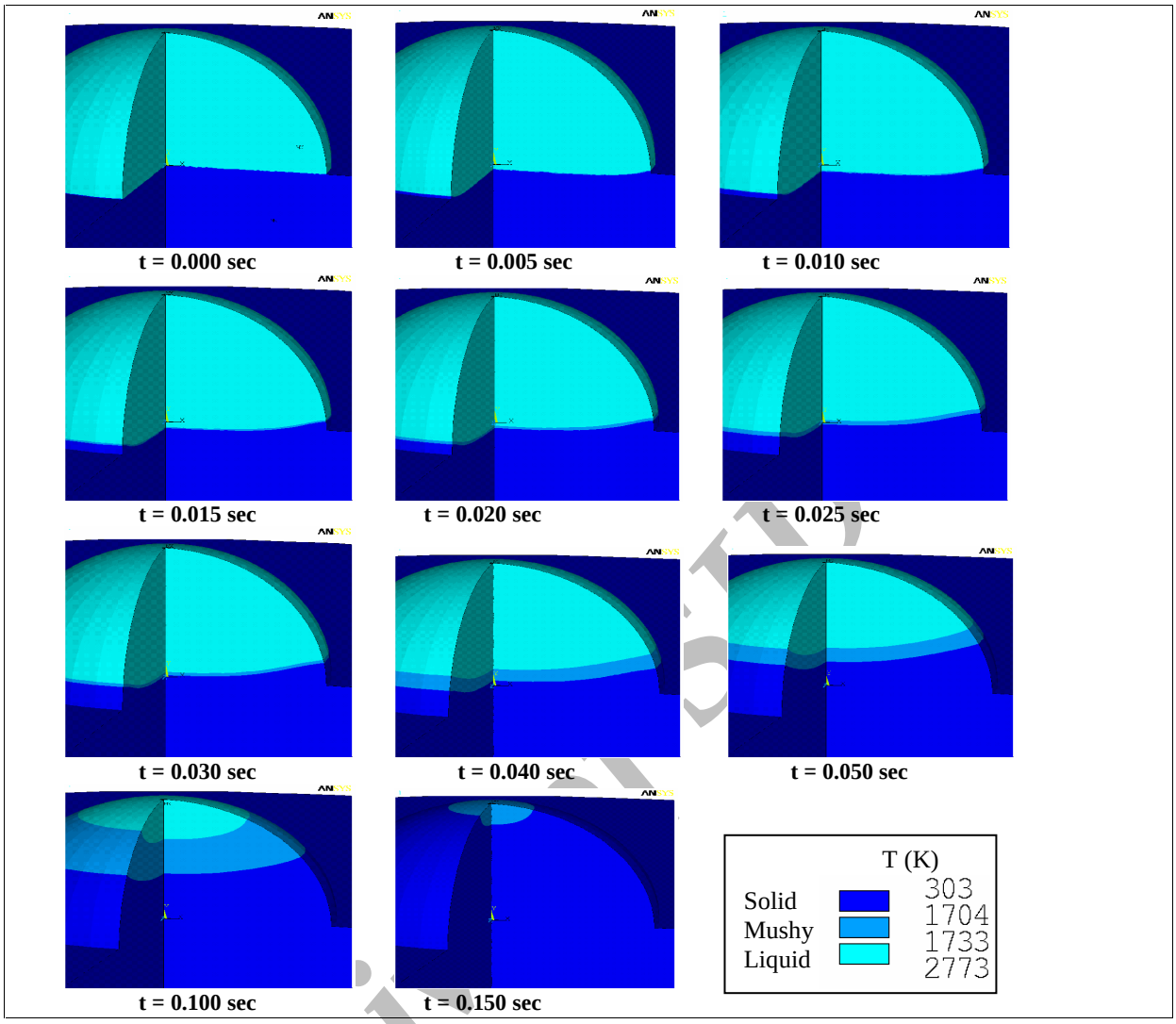

Fig. 11. Phase regions and solidification profile during microcasting process (T_L=1733, T_S=1704)

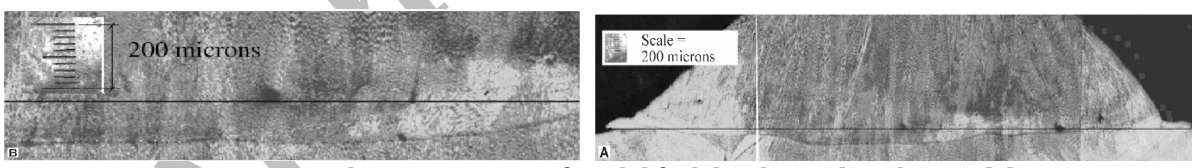

Fig. 12. Typical macrostructure of a solidified droplet on the substrate [6]

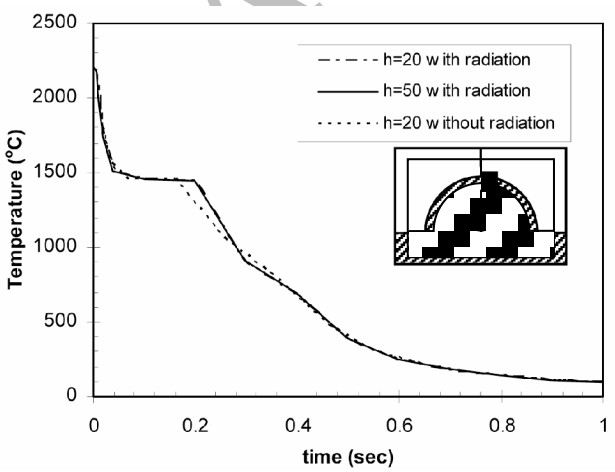

Fig. 13. Boundary effects on the cooling curve of a point on the droplet

Therefore it is expected that it does not mainly affects the structure, while it could effectively reduce residual stresses. To observe that effects measure quantitatively, the position of liquidus temperature is captured with time in the substrate (on the symmetry axis), which is shown in Fig. 16 and 17. Initial temperature of the droplet also directly affects the maximum remelting dept in the substrate. As soon as the droplet becomes in contact with the substrate at time t=0, the substrate begins to remelt under the droplet. The dept of remelting is in the order of 10 μm and increases to a maximum value (a minimum position with respect to y-coordinate). Then the substrate solidifies upward and solidification continues through the droplet. The history of solidification front within the substrate is demonstrated in Fig. 26. It is obvious that more drop heat content (Initial droplet temperature) causes more remelting dept, so that a 300 °C increase in

droplet temperature, results in a significant progress of maximum remelting dept and a 400 °C decrease in droplet temperature makes the droplet disable to relatively remelt the substrate. But in Fig. 17 variation of substrate temperature in the common range has a little effect on the maximum remelting dept.

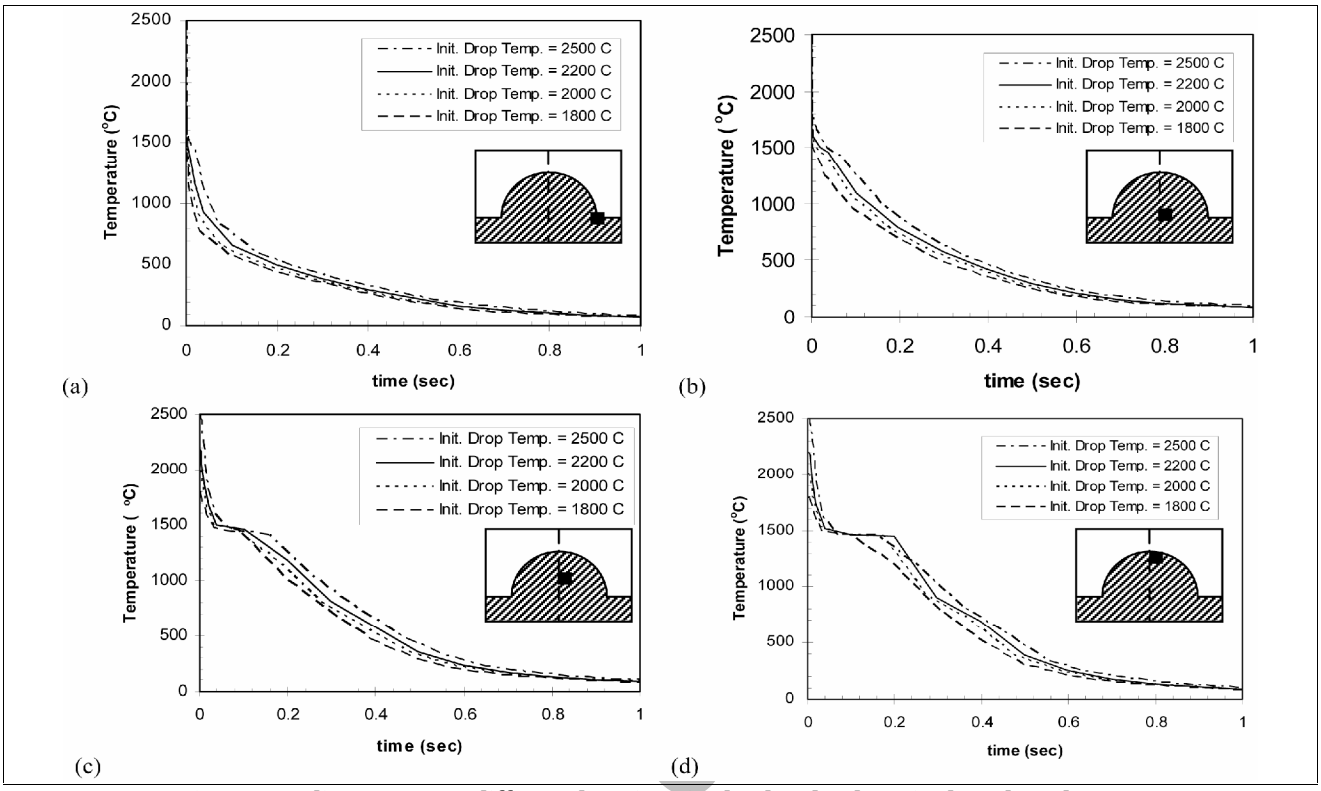

Fig. 14. Cooling curves at different locations in the droplet deposited on the substrate under different conditions of initial drop temperature

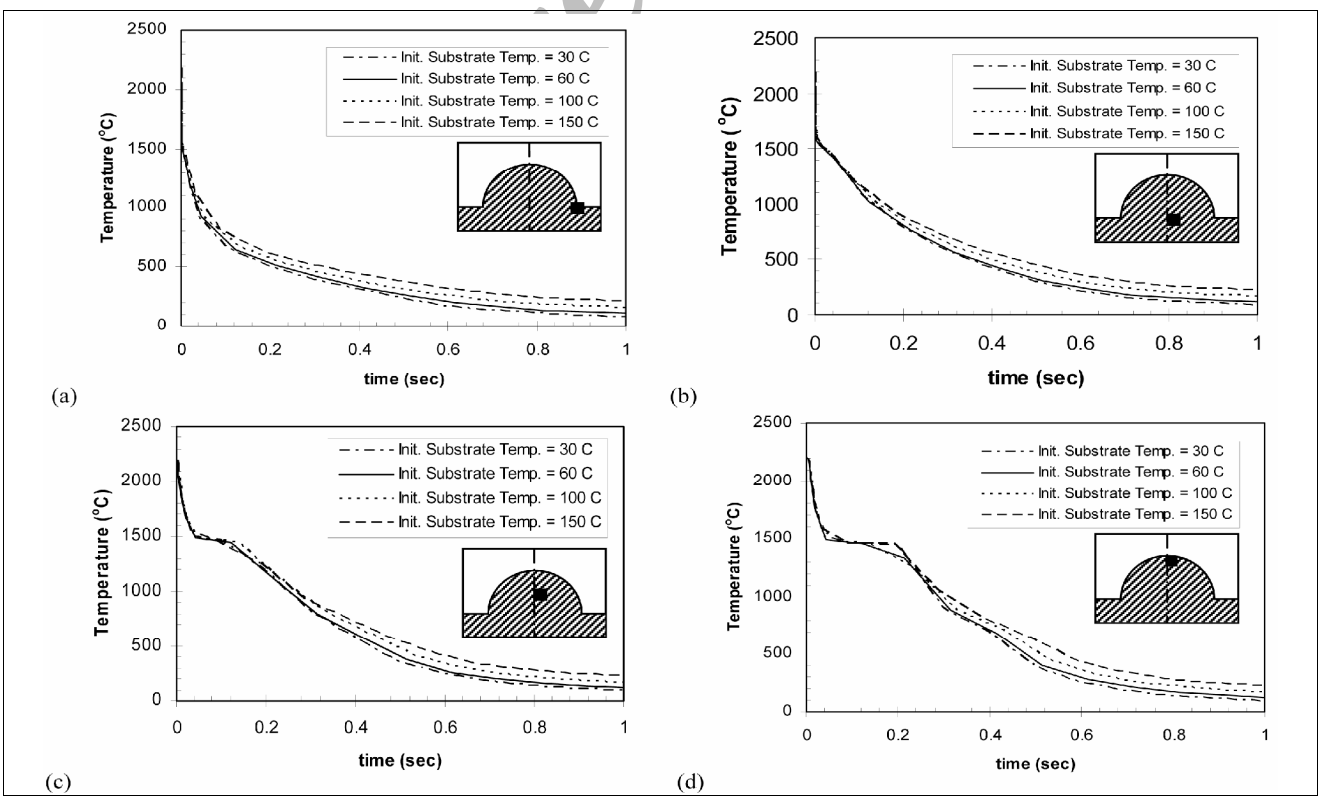

Fig. 15. Cooling curves at different locations in the droplet deposited on the substrate under different conditions of initial substrate temperature

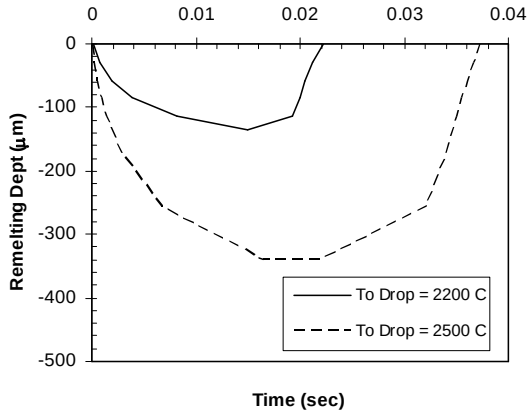

Fig. 16. Remelting dept history in the substrate for different initial drop temperature.

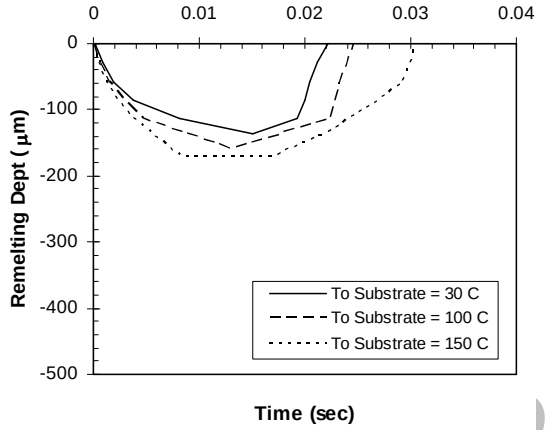

Fig. 17. Remelting dept history in the substrate for different substrate temperature

5. Conclusion

A heat transfer Finite Element Analysis with solidification was performed to investigate microcasting SDM process, trying to improve our insight of the process. The model was verified by available experimental data (Fig. 9). Results in the form of temperature field (Fig. 10), solidification profiles (Fig. 11), cooling curves (Fig. 13 to 15) and remelting dept history curves (Fig. 16 and Fig.17) were obtained. The results help to make a better understanding of microcasting SDM process, as well as some quantitative predictions.

Important issues in microcasting SDM process are cooling rate, substrate remelting and stress buildup. It is concluded that the main parameter which can effectively controls substrate remelting is initial temperature of the droplet (Fig. 16). A useful quantitative reference graph can be made in the form of Fig. 16 to be used for practically adjusting the remelting dept. The droplet falls in a short path between torch and substrate before impinging and it is cooled down slightly from the torch temperature by convection and radiation to the inert atmosphere through the path. This may be a useful help to fine tune the initial temperature by adjusting the path length simply by controlling the height of robot arm. In this case another heat transfer model during the falling of the droplet can give a relation between falling height and droplet temperature at impingement. Therefore, a quantitative relation between torch height and substrate remelting (with constant torch temperature) can be obtained to control the height of the robot arm, producing predefined remelting dept for each drop.

According to the results (Fig. 13) microcasting SDM process does not sensitive to convection and radiation parameters, while convective heat transfer and solidification parameters are dominant. The other issue, stress build up, should be investigated individually, but as a heat transfer study it is concluded that substrate temperature is the main parameter that can be adjust for stress minimization, since it has minor effect on solidification and structure development and slightly promotes substrate remelting. In the real case this parameter is controlled by a heating/cooling system around the substrate part as well as the intervals between drop times. High drop frequency would lead to a heat build up in the part. The geometry of the substrate part becomes important in this case, where, a transient heat transfer model of substrate can predict the substrate temperature for different geometries and drop frequencies.

References

[1] Chin, R.K., Beuth, J.L., Amon, C.H., *"Successive Deposition Of Metals In Solid Freeform Fabrication Processes, Part 1: Thermo Mechanical Models Of Layers And Droplet Columns*", *J. of Manufacturing Science and Engineering*, Vol. 123, Nov. 2001, pp 623-631.

[2] Li, X.C., Stampfl, J., Prinz, F.B., "*Design And Fabrication Of Materials For Laser Shape Deposition Manufacturing*", 44th Int. SAMPE Symposium, L.J.Cohen et al. (eds), Long Beach, Vol. 44(2), May 1999, pp1849-1856.

[3] Schmaltz, K.S., Zarzalejo, L.J., Amon, C.H., *"Molten Droplet Solidification and Substrate Remelting In Microcasting Part II: Parametric Study and Effect Of Dissimilar Materials*, Heat and Mass Transfer, Vol. 35 1999, pp. 17-23.

[4] Vasinonta, A., Beuth, J.L., Griffith, M.L., "*A Process Map for Consistent Build Conditions in the Solid Freeform Fabrication of Thin-Walled Structures*", J. of Manufacturing Science and Engineering, Vol. 123, Nov. 2001, pp. 615-622.

[5] Grylls, Richard, *"Laser Engineered Net Shapes*", Advanced Materials and Processes, v 161, n 1, January, 2003, p 45-46-86.

[6] Zarzalejo, L.J., Schmaltz, K.S., Amon, C.H., *"Molten Droplet Solidification and Substrate Remelting In Microcasting Part I: Numerical Modeling and Experimental Verification*, Heat and Mass Transfer, Vol. 34, 1999, pp. 477-485.

[7] Amon, C.H., Beuth.; J.L., Weiss.; L.E., Merz; R., Prinz, F.B., *"Shape Deposition Manufacturing with Microcasting: Processing, Thermal and Mechanical Issues*", Journal of Manufacturing Science and Engineering, Transactions of the ASME, Vol. 120, No. 3, Aug, 1998, pp. 656-665.

[8] Schmaltz, K.S., Amon, C.H., *"Thermal Issues in Microcasting Shape Deposition Manufacturing"* TMS Annual Meeting, Melt Spinning, Strip Casting and Slab Casting, 1995, pp.145-157.

[9] Amon, C.H.; Schmaltz, K.S.; Merz, R.; Prinz, F.B., "*Numerical and Experimental Investigation of Interface Bonding Via Substrate Remelting of a Impinging Molten Metal Droplet"*, Journal of Heat Transfer, Transactions ASME, v 118, n 1, Feb, 1996, p 164-172.

[10] Chin, R.K., Beuth; J.L., Amon, C.H., *"Thermo Mechanical Modeling of Molten Metal Droplet Solidification Applied to Layered Manufacturing"*, Mechanics of Materials, v 24, n 4, Dec, 1996, p 257-271.

[11] Chin, Richard, K., Beuth, Jack L.; Amon, Cristina H., "*Droplet-level Modeling of Thermal Stresses in Layered Manufacturing Methods*", American Society of Mechanical Engineers (Paper),1996, 14p.

[12] Kovacevic, Radovan; Beardsley, Heather E.; Fan, Honggang, *"Modeling, Sensing and Control of Droplet Based Solid Freeform Fabrication Process*", American Society of Mechanical Engineers, Petroleum Division (Publication) PD, Manufacturing and Services, 1999, 15p.

[13] Fang, M.; Chandra, S.; Park, C.B., "*Remelting and Coalescence of Molten Metal Droplets Deposited on a Plate"*, Proceedings of the ASME Heat Transfer/Fluids Engineering Summer Conference 2004, HT/FED 2004, v 3, Proceedings of the ASME Heat Transfer/Fluids Engineering Summer Conference, HT/FED 2004, 2004, pp. 939-944.

[14] Carter, P.W., "*Advances in Rapid Prototyping and Rapid Manufacturing"*, Proceedings of the Electrical/Electronics Insulation Conference, 2001, pp. 107-114.

[15] Jandric, Z.; Kovacevic, R. ,*Heat Management in Solid Free-Form Fabrication Based on Deposition by Welding*", Proceedings of the Institution of Mechanical Engineers, Part B: Journal of Engineering Manufacture, v 218, n 11, November, 2004, pp. 1525-1540.

[16] Sahu, S.N.; Harikishore, S.; Koria, S.C., *"Solidification Behaviour of Droplets in Spray Deposition*", Powder Metallurgy, v 48, n 3, September, 2005, pp. 270-276.

[17] Chin, R.K., Beuth, J.L. Amon, C.H., "*Successive Deposition of Metals in Solid Freeform Fabrication Processes, Part 2: Thermomechanical Models of Adjacent Droplets"*, J. of Manufacturing Science and Engineering, Vol. 123, Nov. (2001) pp 632-638.

[18] Klingbeil, N.W.; Beuth, J.L.; Chin, R.K.; Amon, C.H., *"Residual Stress-induced Warping in Direct Metal Solid Freeform Fabrication*", International Journal of Mechanical Sciences, v 44, n 1, January, 2002, pp. 57-77.

[19] Costa, L.; Vilar, R.; Reti, T.; Deus, A.M., *"Rapid Tooling by Laser Powder Deposition: Process Simulation Using Finite Element Analysis,* "Acta Materialia, v 53, n 14, August, 2005, pp. 3987-3999.

[20] Flemings, M.C., "*Solidification Processing*", McGraw-Hill Inc., USA, 1974.

[21] Brimacombe, J.K., Samarasekara, I.V., "*CONTINUOUS CASTING", Vol. 2, "Heat Flow, Solidification and Crack Formation",* A publication of the Iron & Steel Society of AIME, USA, 1984.

[22] Harkki, K., Meittinen, J. *"Mathematical Modeling of Copper and Brass Upcasting",* Metallugical and Materials Transaction B, Vol. 30B, Feb. 1999, pp. 75-98.

[23] Voller, V.R., *"A Fixed Grid Numerical Modeling Methodology For Convection-Diffusion Mushy Region Phase-Change Problems*", Int. J. Heat and Mass Transfer, Vol. 30, No. 8, 1987, pp-1709-1719,.

[24] Holman, J.P., "*Heat Transfer*", 8th ed., McGraw-Hill Inc. 1997.

[25] Segerlind, L.J., "*Applied Finite Element Analysis*", 2nd ed., John Wiley & Sons Inc, USA, 1984.

[26] Li, X.C., Golnas, A., Prinz, F., *"Shape Deposition Manufacturing of Smart Metallic Structures with Embedded Sensors*", Proceedings of SPIE - The International Society for Optical Engineering, Vol. 3986, 2000, pp. 160-171.

[27] Zhang, Haiou, Xu, Jipeng; Wang, Guilan, *"Fundamental Study on Plasma Deposition Manufacturing",* Surface and Coatings Technology, v 171, n 1-3, Jul 1, 2003, pp. 112-118.

[28] Beuth, Jack L., Narayan, Shri H., "*Residual Stress-Driven Delamination in Shape Deposited Materials*", American Society of Mechanical Engineers, Applied Mechanics Division, AMD, v 194, Mechanics in Materials Processing and Manufacturing, 1994, pp. 19-34.

[29] Kwak, Yong-Min; Doumanidis, Charalabos, *"Solid Freeform Fabrication by GMA welding: Geometry Modeling, Adaptation and Control*", American Society of Mechanical Engineers, Manufacturing Engineering Division, MED, V.10, 1999, pp. 49-56.

[30] Mughal, M.P.; Fawad, H.; Mufti, R.A.; Siddique, M., *"Deformation Modelling in Layered Manufacturing of Metallic Parts Using Gas Metal Arc Welding: Effect of Process Parameters*", Modelling and Simulation in Materials Science and Engineering, v 13, n 7, Oct 1, 2005, pp. 1187-1204.

[31] Miller, R.S.; Cao, G.; Grujicic, M., "*Monte Carlo Simulation of Three-Dimensional No Isothermal Grain-Microstructure Evolution: Application to LENS rapid Fabrication",* Journal of Materials Synthesis and Processing, V. 9, N. 6, November, 2001, pp. 329-345.

[32] Griffith, M.L.; Ensz, M.T.; Puskar, J.D.; Robino, C.V.; Brooks, J.A.; Philliber, J.A.; Smugeresky, J.E.; Hofmeister, W.H., "*Understanding the Microstructure and Properties of Components Fabricated by Laser Engineered Net Shaping (LENS)",* Materials Research Society Symposium - Proceedings, V. 625, 2000, pp. 9-20.